Journal of Molecular Cell Biology (2023), 15(5), mjad027 https://doi.org/10.1093/jmcb/mjad027
Published online May 18, 2023

Article

Cellular gp96 upregulates AFP expression by blocking NR5A2 SUMOylation and ubiquitination in hepatocellular carcinoma

Liyuan Qian[1], Zhentao Liang[1,2], Zihao Wang[1,2], Jiuru Wang[1,2], Xin Li[1], Jingmin Zhao[3], Zihai Li[4], Lizhao Chen[1], Yongai Liu[1,2], Ying Ju[1], Changfei Li[1,*], and Songdong Meng[1,2,*]

[1] Key Laboratory of Pathogen Microbiology and Immunology, Institute of Microbiology, Chinese Academy of Sciences, Beijing 100101, China
[2] University of Chinese Academy of Science, Beijing 100049, China
[3] Department of Pathology and Hepatology, The Fifth Medical Centre, Chinese PLA General Hospital, Beijing 100039, China
[4] Pelotonia Institute for Immuno-Oncology, The Ohio State University Comprehensive Cancer Center—The James, Columbus, OH 43210, USA
* Correspondence to: Songdong Meng, E-mail: mengsd@im.ac.cn; Changfei Li, E-mail: lichangfei2006@163.com

Edited by Hua Lu

Alpha-fetoprotein (AFP) is the most widely used biomarker for the diagnosis of hepatocellular carcinoma (HCC). However, a substantial proportion of HCC patients have either normal or marginally increased AFP levels in serum, and the underlying mechanisms are not fully understood. In the present study, we provided *in vitro* and *in vivo* evidence that heat shock protein gp96 promoted AFP expression at the transcriptional level in HCC. NR5A2 was identified as a key transcription factor for the AFP gene, and its stability was enhanced by gp96. A further mechanistic study by co-immunoprecipitation, GST pull-down, and molecular docking showed gp96 and the SUMO E3 ligase RanBP2 competitively binding to NR5A2 at the sites spanning from aa 507 to aa 539. The binding of gp96 inhibited SUMOylation, ubiquitination, and subsequent degradation of NR5A2. In addition, clinical analysis of HCC patients indicated that gp96 expression in tumors was positively correlated with serum AFP levels. Therefore, our study uncovered a novel mechanism that gp96 regulates the stability of its client proteins by directly affecting their SUMOylation and ubiquitination. These findings will help in designing more accurate AFP-based HCC diagnosis and progression monitoring approaches.

Keywords: gp96, AFP, NR5A2, RanBP2, SUMOylation

Introduction

Alpha-fetoprotein (AFP), a 70-kDa glycoprotein, is the main serum protein produced during fetal life (Deutsch, 1991). Unlike other members of the serum-albumin family, the AFP gene is transcriptionally silent in the adult liver but is reactivated in hepatocellular carcinoma (HCC), where elevated serum AFP levels have been found in ∼70%–85% of HCC patients (Galle et al., 2019). Since serum AFP is mainly produced by hepatic tumor cells, a concentration of 20 ng/ml is generally used as a pathological threshold value, and >400 ng/ml is usually considered diagnostic for HCC (Sauzay et al., 2016; Galle et al., 2019). Although new oncologic markers have been discovered, AFP remains the most widely used biomarker in HCC diagnosis (Sauzay et al., 2016; Galle et al., 2019).

Several regulatory mechanisms of pathological AFP expression have been reported in HCC (Sauzay et al., 2016). Numerous transcription factors are crucial for the regulation of the AFP promoter (Kajiyama et al., 2006; Peterson et al., 2011; Sauzay et al., 2016). Human AFP gene comprises five regulatory regions: a tissue-specific promoter, a repressor upstream of the promoter, and three enhancers located 2.5, 5.0, and 6.5 kb upstream of the promoter, respectively (Bernier et al., 1993; Sauzay et al., 2016). Potential AFP transcription factors include hepatocyte nuclear factor-1 (HNF1), liver receptor homolog-1 [LRH-1, also known as α1-fetoprotein transcription factor or nuclear receptor subfamily 5 group A member 2 (NR5A2)], retinoid X receptor (RXR), CAAT/enhancer binding

Received November 20, 2022. Revised April 20, 2023. Accepted April 24, 2023.

protein (C/EBP), homeobox protein NK-2 (Nkx2.8), zinc-fingers and homeoboxes 2 (Zhx2), and zinc finger and BTB domain containing 20 (Zbtb20) (Bernier et al., 1993; Kajiyama et al., 2006; Peterson et al., 2011; Sauzay et al., 2016). Zhx2 and Zbtb20 bind specifically to the AFP promoter and inhibit its activity; their levels are increased with the decrease in AFP expression after birth (Xie et al., 2008; Peterson et al., 2011). AFP expression could also be regulated post-transcriptionally by miRNAs, including miRNA-122, miRNA-620, miRNA-1236, miRNA-1270, and miRNA-329, which directly target the 3′-UTR of AFP mRNA (Kojima et al., 2011; Gao et al., 2015). In addition, epigenetic regulation, such as methylation or acetylation, of the AFP gene also influences AFP expression (Chen et al., 2020; Xue et al., 2020). Nevertheless, serologic surveillance showed that a significant proportion (∼15%–30%) of HCC patients have either normal or minimally increased AFP levels (Gurakar et al., 2018). Meanwhile, other liver diseases, such as hepatitis and cirrhosis, may also lead to elevated serum AFP levels. Therefore, the exact regulatory mechanisms of AFP expression in HCC are not well understood and need further investigation (Sauzay et al., 2016; Galle et al., 2019).

Heat shock protein (HSP) gp96 is the most abundant protein in the endoplasmic reticulum (ER) (Wu et al., 2016). Similar to most HSPs, gp96 acts as a molecular chaperone in protein folding and facilitates the degradation of misfolded proteins. Unlike its cytosolic counterpart HSP90, gp96 has a relatively strict binding selectivity and only binds to certain client proteins, including Toll receptor (Toll-like receptors), the majority of α and β integrin subunits, the Wnt co-receptor LRP6, GARP, insulin-like growth factor, binding immunoglobulin protein, epidermal growth factor receptor-2 (HER2), and uPAR (Liu et al., 2010; Hong et al., 2013; Li et al., 2015; Wu et al., 2015, 2016; Hou et al., 2015b; Ansa-Addo et al., 2016; Marzec et al., 2016; Duan et al., 2021). These client proteins are involved in balancing cancer-induced ER stress responses and regulating inflammation in the tumor microenvironment (Marzec et al., 2012). An elevated level of gp96 correlates with the development, invasion, and metastasis of tumors, which validates the pro-oncogenic function of cellular gp96 (Li et al., 2015; Wu et al., 2015, 2016; Hou et al., 2015b; Ansa-Addo et al., 2016; Duan et al., 2021). Furthermore, cellular and cell membrane gp96 has been shown to promote anti-apoptotic characteristics and metastasis of HCC via the interaction with p53 and uPAR, indicating the association of high gp96 expression levels with tumor metastasis and recurrence (Wu et al., 2015; Hou et al., 2015b; Cho et al., 2022; Pugh et al., 2022).

The present study aimed to comprehensively examine the effects of gp96 on AFP expression and serum AFP levels in HCC by generating hepatic gp96 knockout (gp96KO) mice and performing clinical sample analysis. The gp96-mediated regulatory network was further dissected. The results uncovered a novel regulatory pathway of AFP expression and suggested that detection of gp96 levels may increase the sensitivity of HCC diagnosis by the AFP test.

Results

Hepatic knockout of gp96 dramatically decreases AFP levels in DEN-induced HCC

In this study, we used the well-established diethylnitrosamine (DEN)-induced HCC model, where liver-specific gp96KO mice and Het mice were intraperitoneally injected with DEN to induce hepatic tumors (Rachidi et al., 2015). Deletion of gp96 (*Hsp90b1*) in the liver of gp96KO mice was confirmed by real-time PCR and western blotting (Figure 1A; Rachidi et al., 2015). Eight months after DEN injection, both gp96KO and Het mice developed visible liver tumors; tumor histological features were shown by hematoxylin and eosin (HE) staining (Figure 1B; Rachidi et al., 2015). Compared to the normal liver tissues from phosphate-buffered saline (PBS)-treated Het mice, liver tumors from DEN-induced Het mice showed a drastic increase in gp96 and AFP levels (Figure 1C). Consistent with a previous study, fatty nodules were observed in liver tumor tissue sections of gp96KO mice (Supplementary Figure S1A; Rachidi et al., 2015). gp96KO mice showed the decreased tumor weight and lower tumor burden compared to Het mice under DEN treatment (Figure 1D). Global gene expression in liver tumor tissues of DEN-treated gp96KO and Het mice was studied by transcriptome analysis. Compared to the Het group, the gp96KO group had 5413 upregulated and 4488 downregulated genes (Figure 1E; Supplementary Additional file 1; log2(fold change) $>$ 0.5), among which AFP expression was reduced by ∼2.488-fold. The decreased AFP gene expression was confirmed by real-time PCR (Figure 1F), western blotting (Figure 1G), and immunohistochemistry (IHC) analysis (Figure 1H).

Cellular gp96 promotes AFP expression mainly through the transcription factor NR5A2 in hepatoma cells

Two hepatoma cell lines, Huh7 and HepG2, with stable knockdown of gp96 were used to determine gp96-mediated AFP expression. Compared to the mock, knockdown of gp96 caused an obvious decrease in AFP mRNA and protein levels (Figure 2A and B). gp96 knockdown also caused a pronounced decrease in AFP levels by 98% and 95% in the supernatant of Huh7 and HepG2 cells, respectively (Figure 2C). In contrast, overexpression of gp96 in Huh7 cells increased both cellular AFP levels (Figure 2D and E) and AFP secretion (Figure 2F). Overall, the data suggested that gp96 promotes AFP expression at the transcriptional level.

The effects of gp96 on the expression of AFP transcription factors

The potential binding sites of AFP transcription factors in the AFP promoter are shown in Figure 3A (Bernier et al., 1993; Kajiyama et al., 2006; Peterson et al., 2011; Sauzay et al., 2016). As shown in Figure 3B and C, knockdown of gp96 caused a sharp decrease in HNF1, HNF4, and C/EBPα but an increase in Nkx2.8 mRNA and protein levels, while gp96 knockdown only decreased NR5A2 protein level but did not affect its mRNA level. Furthermore, an AFP promoter luciferase reporter assay

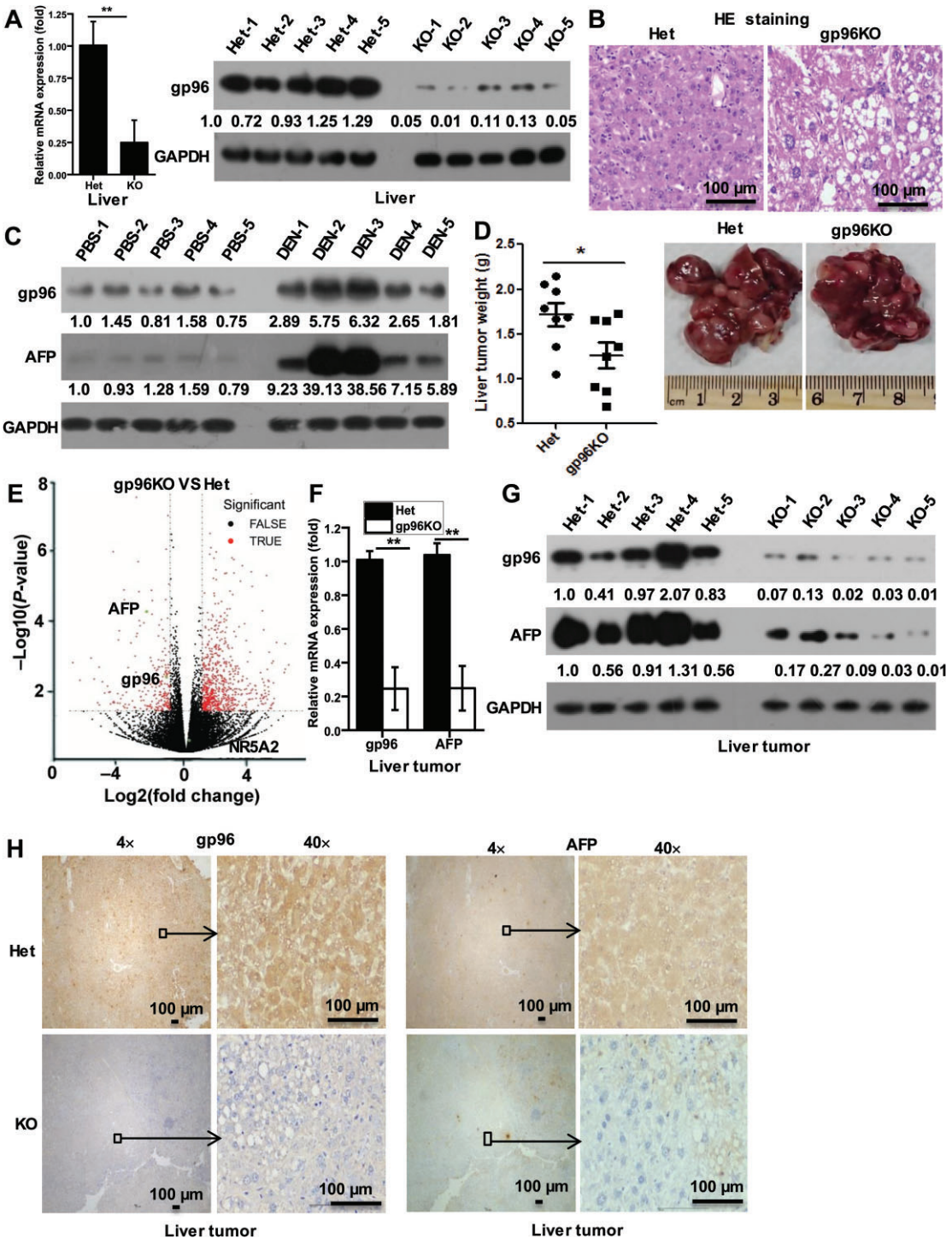

Figure 1 AFP expression in the liver tumors of hepatic gp96KO mice. (**A**) Real-time PCR and western blot analysis for gp96 mRNA and protein levels, respectively, in normal liver tissues from Het and gp96KO mice ($n = 5$/group). (**B**) Representative HE staining images of liver tumors from DEN-treated Het and gp96KO mice. (**C**) gp96 and AFP protein levels in normal liver or liver tumor tissues from PBS-treated or DEN-treated Het mice, respectively. (**D**) Mass of liver tumors from Het and KO mice after 8 months of DEN treatment. (**E**) Microarray volcano map of differentially expressed genes in hepatic tumors from DEN-treated gp96KO and Het mice. (**F** and **G**) gp96 and AFP mRNA and protein levels in liver tumors from DEN-treated Het and gp96KO mice ($n = 5$/group). (**H**) IHC analysis for gp96 and AFP expression in paraffin sections of liver tumors from DEN-treated Het and gp96KO mice. $^{**}P < 0.01$.

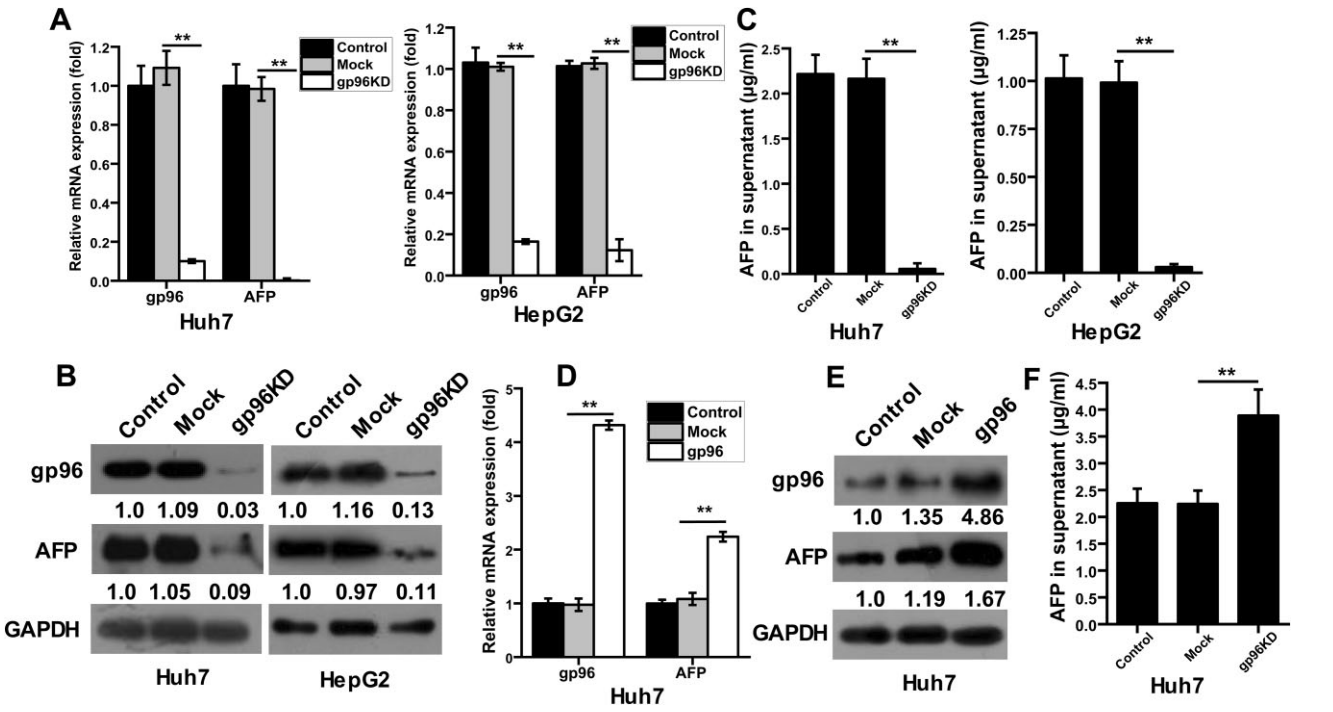

Figure 2 Effects of gp96 knockdown or overexpression on AFP levels in hepatoma cell lines. (**A**–**C**) Huh7 and HepG2 cells were stably transfected with gp96 shRNA (gp96KD) or luciferase shRNA (mock), or untransfected (control). (**A** and **B**) Cellular gp96 and AFP mRNA and protein levels were detected. (**C**) AFP levels in cell supernatant were analysed by ELISA. (**D**–**F**) Huh7 cells were stably transfected with gp96 vector or empty vector (mock) or untransfected (control). Cellular gp96 and AFP levels and AFP levels in cell supernatant were measured. Data are presented as mean ± SD from three independent experiments. $^{**}P < 0.01$ compared to the mock.

was performed to determine the key transcription factors involved in gp96-induced AFP expression. As shown in Figure Figure 3D and E, mutations within the binding sites of Nkx2.8 or NR5A2/HNF4 significantly suppressed AFP promoter activity in Huh7 cells, while mutations within the binding sites of HNF1 only led to a slight decrease in AFP promoter activity. In accordance, gp96 knockdown-induced decrease in AFP promoter activity was only mildly affected by mutations in HNF1 binding sites but was abolished by mutations in Nkx2.8 or NR5A2/HNF4 binding sites (Figure 3D and E). Nkx2.8, NR5A2, and HNF4 were then selected for RNAi treatment. Only NR5A2 siRNA treatment largely restored the promoter activity suppressed by gp96 knockdown (Figure 3F; Supplementary Figure S2). NR5A2 siRNA treatment also minimized the reduction of AFP expression caused by gp96 knockdown (Figure 3G). Collectively, these data suggested that cellular gp96 regulates AFP expression mainly via NR5A2.

Cellular gp96 interacts with NR5A2 and enhances its stability

Next, the effect of gp96 on the expression of NR5A2 was determined. A sharp increase in NR5A2 protein level (~3.6 folds) but not its mRNA level was detected in gp96-transfected Huh7 cells compared to mock cells (Figure 4A and B). In addition, the gp96-mediated increase in NR5A2 levels was gp96 dose-dependent (Figure 4C). Conversely, a drastic reduction of 87% in NR5A2 protein level, but not in its mRNA level, was observed in Huh7-gp96KD cells (Figure 4D and E). The decrease in NR5A2 protein levels was also observed in DEN-induced liver tumors of gp96KO mice (Supplementary Figure S3; Rachidi et al., 2015). As shown in Figure 4F, gp96 knockdown caused a dramatic reduction in the protein stability of NR5A2.

As illustrated in Figure 4G, co-immunoprecipitation (co-IP) results showed that endogenous gp96 is associated with NR5A2 in Huh7 cells. To identify the interaction regions between gp96 and NR5A2, GST-tagged full-length gp96, its N-terminal, middle, and C-terminal domain fragments, GST-NR5A2, and His-gp96 were expressed (Supplementary Figure S4A–C). GST pull-down results demonstrated that full-length gp96 and its C-terminal domain were able to directly interact with NR5A2 (Figure 4H–J).

Cellular gp96 inhibits the interaction of RanBP2 with NR5A2 and reduces RanBP2-mediated NR5A2 SUMOylation and subsequent ubiquitination

Knockdown of gp96 in Huh7 cells significantly increased NR5A2 ubiquitination, while gp96 overexpression suppressed NR5A2 ubiquitination dramatically (Figure 5A). Since post-transcriptional processing in nuclear receptors of the NR5A subfamily mainly occurs via SUMOylation, we quantified SUMO1, SUMO2/3, and their related conjugates (Liu et al., 2021a). Our results showed that knockdown or overexpression of gp96 in Huh7 cells affected protein SUMOylation via SUMO1 but not via SUMO2/3 (Supplementary Figure S5A and B). Knockdown

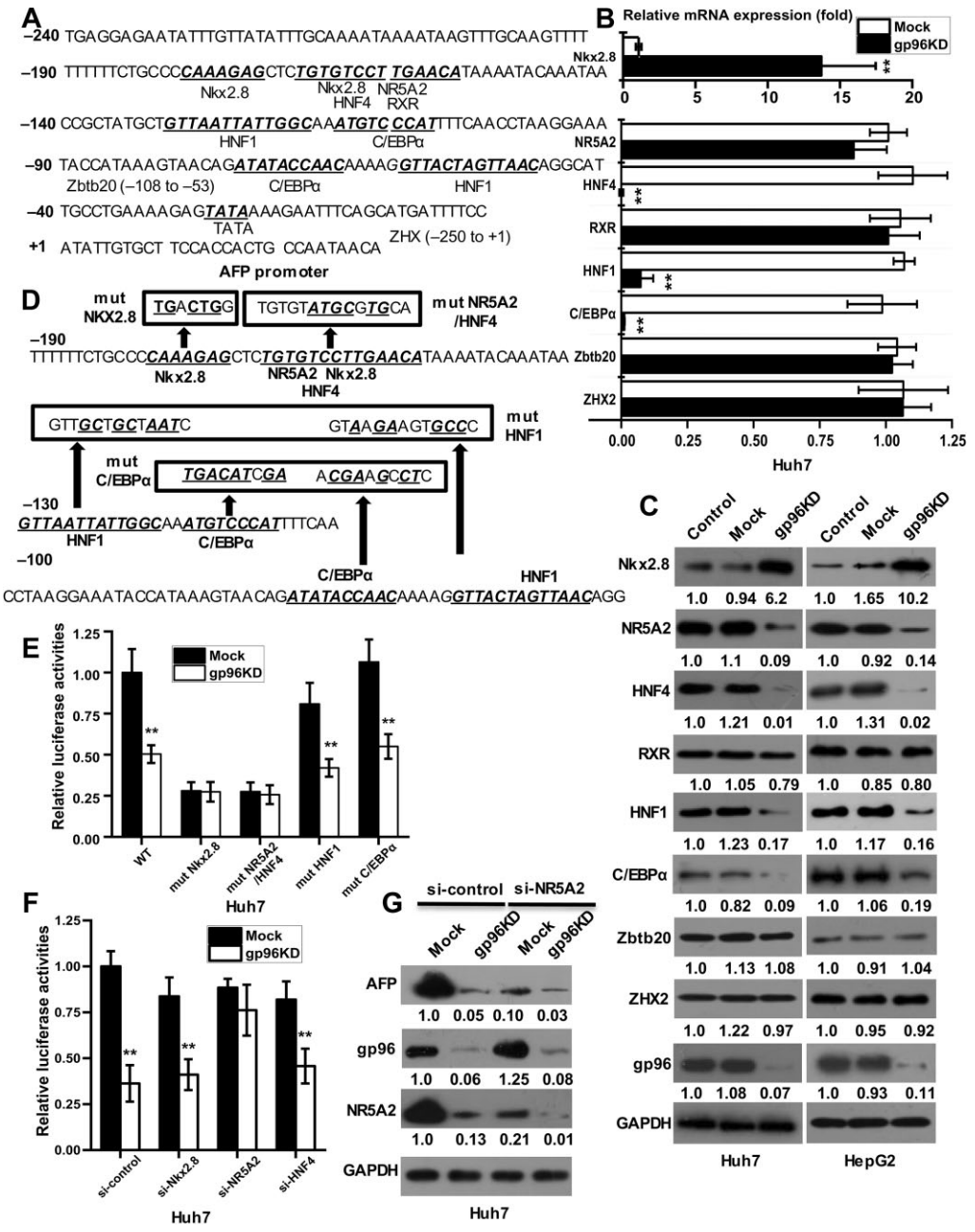

Figure 3 Identification of NR5A2 as a key transcription factor in gp96-induced AFP expression. (**A**) The putative binding sites in the AFP promoter (−240/+29) for its transcription factors are indicated using italics, bold letters, and underscores. (**B** and **C**) The mRNA and protein expression levels of AFP transcription factors in Huh7 or HepG2 cells stably transfected with gp96 shRNA (gp96KD) or luciferase shRNA (mock). (**D**) The mutated binding sites in the AFP promoter for its transcription factors are indicated using italics and bold letters in boxes. (**E**) Huh7-gp96KD or mock cells were co-transfected with pRL-TK and the pGL3-Basic construct containing wild-type (WT) or mutant AFP promoter (pAFP-Luci) with mutated binding site for Nkx2.8, NR5A2/HNF4, HNF1, or C/EBPα, respectively. After 48 h, luciferase activities were measured. The luciferase activity of mock cells transfected with WT pAFP-Luci was set as 1.0. (**F**) Huh7-gp96KD and mock cells were co-transfected with control siRNA (si-control) or siRNAs against Nkx2.8 (si-Nkx2.8), NR5A2 (si-NR5A2), or HNF4 (si-HNF4), pAFP-Luci, and pRL-TK. After 48 h, luciferase activities were examined. The luciferase activity of mock cells transfected with si-control was set as 1.0. (**G**) Huh7-gp96KD and mock cells were transfected with si-NR5A2 or si-control, and cellular protein levels were determined. Data are presented as mean ± SD from three independent experiments. *$P < 0.05$ and **$P < 0.01$ compared to the mock.

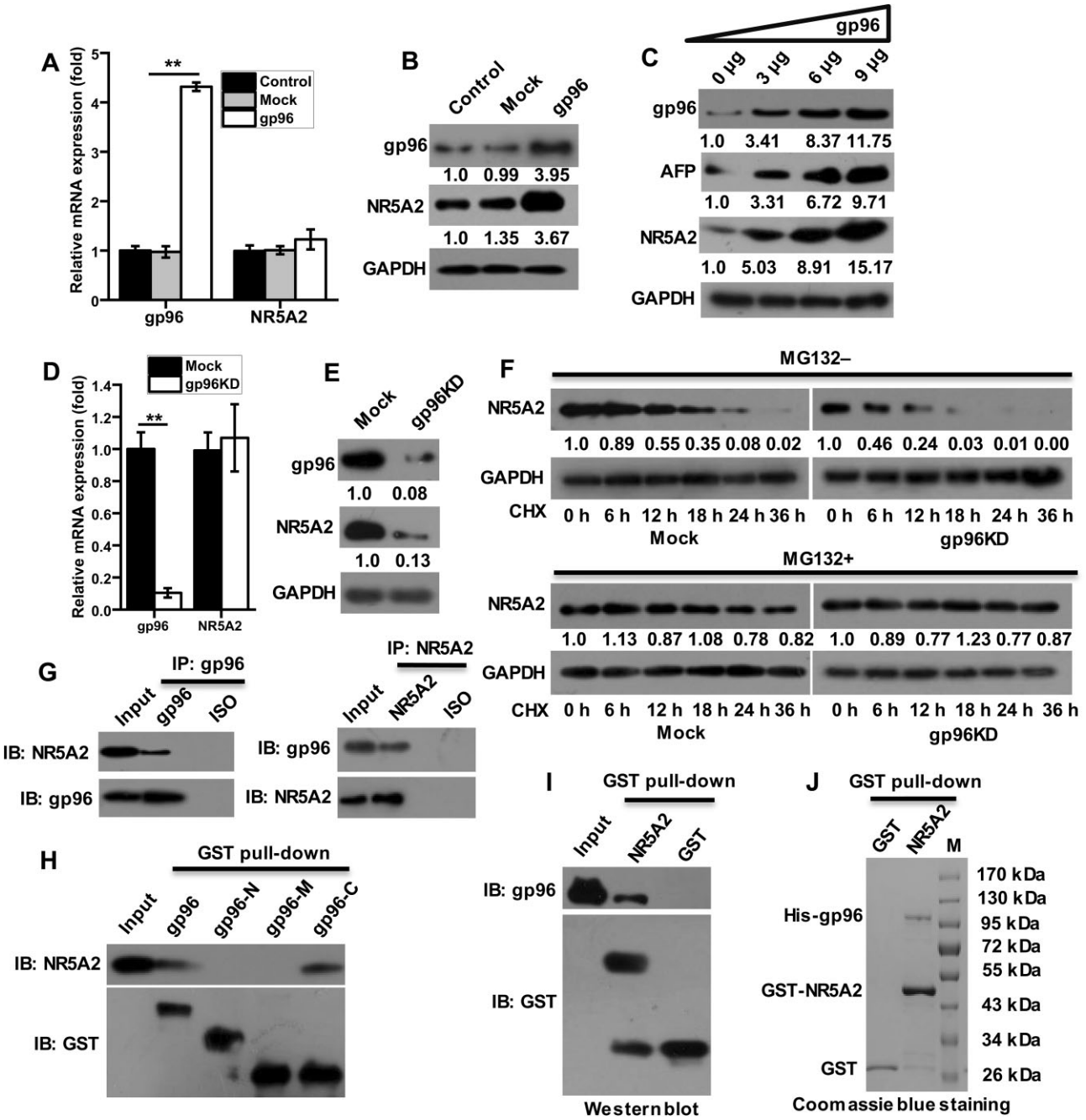

Figure 4 Effects of cellular gp96 on NR5A2 protein stability and their interaction. (**A**, **B**, **D**, and **E**) gp96 and NR5A2 mRNA and protein levels in Huh7 cells with gp96 overexpression (**A** and **B**) or gp96 knockdown (**D** and **E**). (**C**) Huh7 cells were transfected with increasing amount (0, 3, 6, and 9 μg) of pcDNA3.1-gp96. After 48 h, cellular protein levels were determined. (**F**) Huh7-gp96KD or mock cells were treated with 50 μM CHX alone or together with 20 μM MG132. NR5A2 protein levels at the indicated time points were analysed. (**G**) Huh7 cell lysates were used for co-IP experiments with anti-gp96 or anti-NR5A2 monoclonal antibody and IgG as the isotype (ISO) control. The immunoprecipitates were immunoblotted with specific antibodies as indicated. (**H**) Huh7 cell lysates were incubated with equal amounts of GST-tagged gp96 (aa 22–803), gp96-N (aa 22–376), gp96-M (aa 337–594), or gp96-C (aa 561–803) for 3 h, followed by incubation with GST beads overnight at 4°C. The pull-down materials were immunoblotted for NR5A2. (**I**) Huh7 cell lysates were incubated with GST-NR5A2 (aa 299–536) or GST protein, and the GST pull-down materials were immunoblotted for gp96. (**J**) GST-NR5A2 (aa 299–536) or GST protein was incubated with recombinant His-gp96, and the GST pull-down materials were subjected to Coomassie blue analysis. Data are presented as mean ± SD from three independent experiments. $^{**}P < 0.01$ compared to the mock.

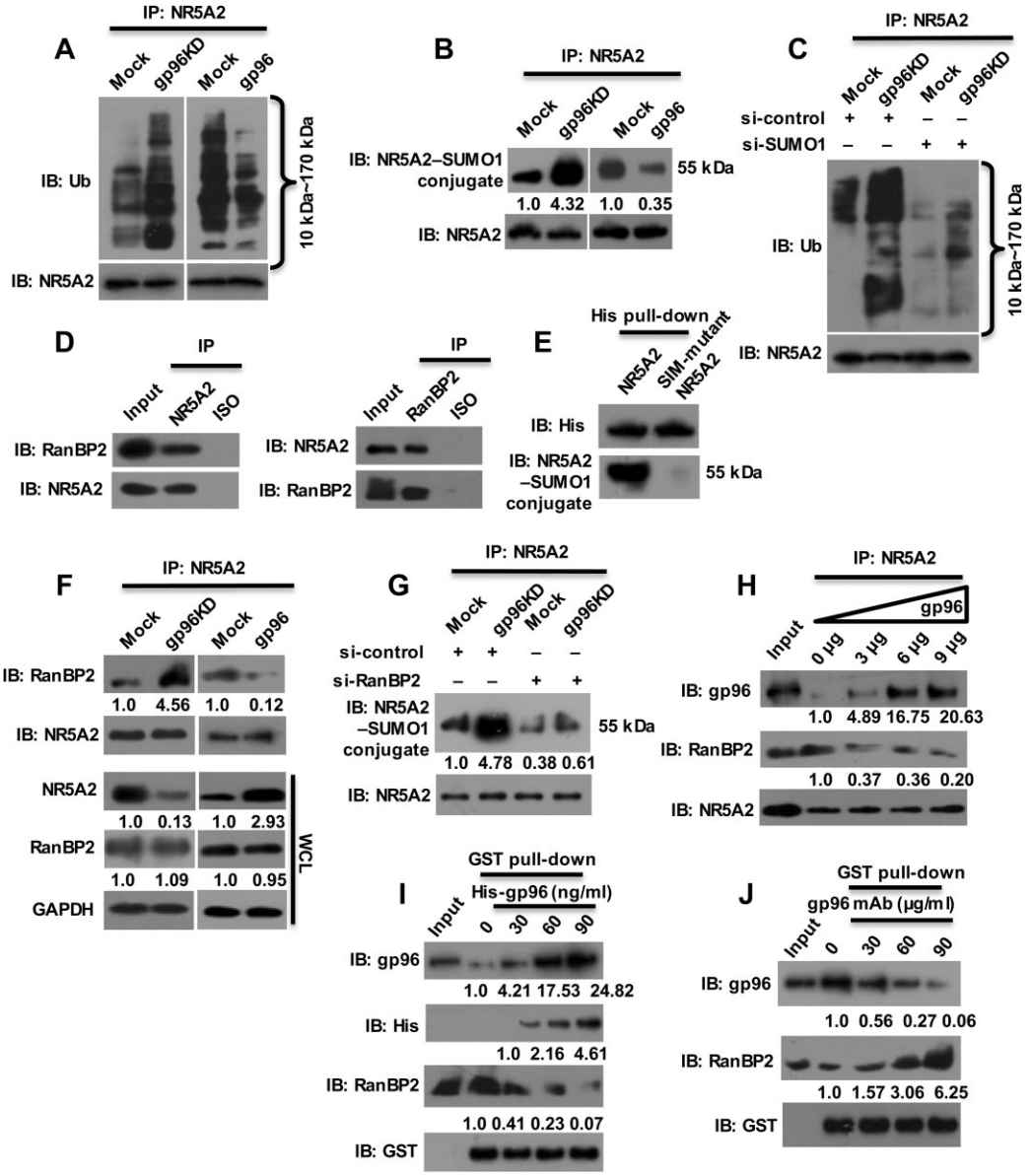

Figure 5 Regulation of RanBP2-mediated NR5A2 SUMOylation and subsequent ubiquitination by gp96. (**A** and **B**) Huh7-gp96KD, Huh7-gp96, or mock cells were exposed to 20 μM MG132 or 20 μM N-ethylmaleimide for 6 h before lysis. NR5A2 protein was immunoprecipitated and immunoblotted for ubiquitin (**A**) or SUMO1 (**B**). (**C**) Huh7-gp96KD and mock cells were transfected with si-SUMO1 or si-control. After 48 h, cells were lysed, and NR5A2 ubiquitination was analysed. (**D**) Huh7 cell lysates were used for co-IP experiments with anti-NR5A2 (left) or anti-RanBP2 (right) antibody and IgG as the ISO control. The immunoprecipitates were immunoblotted with specific antibodies as indicated. (**E**) Huh7 cells were transfected with pcDNA3.1-His-WT NR5A2 or pcDNA3.1-His-SIM mutant NR5A2. After 48 h, cell lysates were incubated with Ni-NTA Sepharose beads for 2–3 h and then immunoblotted for His and SUMO1. (**F**) NR5A2 protein was immunoprecipitated from lysates of Huh7-gp96KD, Huh7-gp96, or mock cells and immunoblotted for RanBP2. Whole-cell lysates (WCL) were also blotted for the respective proteins. (**G**) Huh7-gp96KD and mock cells were transfected with si-RanBP2 or si-control. After 48 h, NR5A2 was immunoprecipitated from cell lysates and immunoblotted for SUMO1. (**H**) Huh7 cells were transfected with increasing amount (0, 3, 6, and 9 μg) of pcDNA3.1-gp96. After 48 h, NR5A2 was immunoprecipitated from cell lysates and immunoblotted for RanBP2. (**I** and **J**) Huh7 cell lysates were incubated with the indicated amounts of His-gp96 (**I**) or gp96 antibody (**J**) and equal amounts of GST-NR5A2 for 3 h, followed by incubation with GST beads overnight. The pull-down materials were immunoblotted for gp96, His, RanBP2, and GST. All experiments were performed at least twice with similar results.

of gp96 promoted NR5A2 SUMOylation by SUMO1 modification, whereas overexpression of gp96 inhibited its SUMOylation (Figure 5B). Moreover, gp96 knockdown-induced NR5A2 ubiquitination was largely attenuated by SUMO1 siRNA (Figure 5C; Supplementary Figure S5C), suggesting that SUMO1 SUMOylation is involved in NR5A2 ubiquitination.

To identify the potential SUMO1 E3 ligase, liquid chromatography–tandem mass spectrometry was performed on NR5A2-associated proteins (Supplementary Additional file 2). Among the detected proteins, the nucleoporin RanBP2 has been reported to possess SUMO1 E3 ligase activity (Pichler et al., 2002; Reverter and Lima, 2005). Co-IP results validated the interaction of NR5A2 with RanBP2 (Figure 5D). Moreover, mutation of SUMO-interacting motif (SIM) within NR5A2 almost completely removed its SUMOylation by SUMO1 (Figure 5E), suggesting that the SUMO1 E3 ligase activity of RanBP2 is SIM-dependent. It was found that their interaction was enhanced in gp96 knockdown cells and suppressed by gp96 overexpression (Figure 5F). However, gp96 knockdown did not affect RanBP2 levels (Supplementary Figure S6). Similarly, gp96 knockdown increased the SUMOylation of NR5A2, which was inhibited by RanBP2 RNAi (Figure 5G; Supplementary Figure S5D). Cellular gp96 inhibited the interaction of NR5A2 with RanBP2 in a dose-dependent manner (Figure 5H). GST pull-down results further demonstrated that gp96 and RanBP2 competitively bound to NR5A2 in a dose-dependent manner (Figure 5I and J).

A similar regulation was observed for the RanBP2 substrate DNA topoisomerase 2-alpha (TOP2A) that could bind to gp96 (Supplementary Figure S7A–C and E; Dawlaty et al., 2008) but not for histone deacetylase 4 (HDAC4), a RanBP2 substrate that could not bind to gp96 (Supplementary Figure S7A, B, D, and F; Kirsh et al., 2002). Altogether, our results indicated that cellular gp96 interacts with its client protein NR5A2, which might specifically block the binding of its SUMO1 E3 ligase RanBP2, thereby suppressing the RanBP2-mediated SUMOylation and subsequent ubiquitination of NR5A2.

The binding sites in NR5A2 overlap for gp96 and RanBP2

Molecular docking was performed with ZDOCK Server (version 3.0.2) on crystal structures obtained from PDB (Pierce et al., 2011). The structural model of full-length NR5A2 has a highly conserved DNA-binding domain (DBD), a conserved 12-α-helical bundle ligand-binding domain (LBD), and a SIM (Seacrist et al., 2020; Liu et al., 2021a). NR5A2 LBD (aa 299–536) was docked and modeled in complex with gp96 (aa 48–754) or RanBP2 (aa 2631–2711) (Figure 6A and B; Supplementary Additional file 3; Huck et al., 2017; Seacrist et al., 2020). It was found that the potential binding sites for gp96 and RanBP2 in NR5A2 span from aa 507 to aa 536 (Figure 6C). As shown in Figure 6D, gp96 interacts with the region of aa 515–536 and RanBP2 binds to the region of aa 507–536. These two regions in NR5A2 were highly overlapped. Both co-IP and His pull-down results demonstrated that truncated NR5A2 (aa 299–506Δ507–536), with depletion of the binding sites, lost its capacity to interact with gp96 or RanBP2 (Figure 6E–G; Supplementary Figure S8). These data verified that the aa 507–536 sequence of NR5A2 is necessary for its binding to both gp96 and RanBP2.

Table 1 gp96 expression levels and clinical characteristics of 63 patients with primary HCC.

Characteristic	gp96 expression		*P*-value
	Low (13/63)	High (50/63)	
Age (years)			0.5018
<50	6	18	
≥50	7	32	
Gender			0.2699
Male	12	38	
Female	1	12	
Tumor size			0.5078
<3 cm	5	14	
≥3 cm	8	36	
Tumor number			0.739
=1	8	35	
>1	5	15	
HBsAg			0.1893
Positive	6	33	
Negative	7	17	
HBcAg			0.8006
Positive	1	5	
Negative	12	45	
T stage			0.2063
I–II	1	0	
III–IV	12	50	
Differentiation grade			0.631
Well differentiated	0	3	
Moderatedly differentiated	12	42	
Poorly differentiated	1	5	
Extrahepatic spread			NA
Yes	0	0	
No	13	50	
Recurrence			NA
Positive	0	0	
Negative	13	50	

gp96 expression in liver tumors correlates with serum AFP levels in HCC patients

To address the clinical correlation of tumor gp96 expression and serum AFP levels in HCC patients, we analysed gp96 expression in 63 primary liver tumors by IHC (Figure 7A and Table 1). IHC staining of intracellular gp96 in liver tissues was shown as faint/medium/strong and quantitatively scored as category 1+/2+/3+, respectively (Hicks and Tubbs, 2005). As shown in Figure 7B, gp96 expression levels were positively correlated with serum AFP levels in HCC patients ($R^2 = 10.177$; $P = 0.001422$). In addition, patients with elevated gp96 expression also displayed higher serum AFP levels (Figure 7C; all $P < 0.01$).

Discussion

In this study, we investigated the regulation of AFP expression by gp96 in HCC. First, comparative transcriptome analysis of DEN-induced liver tumors from gp96KO and Het mice showed that cellular gp96 increased AFP expression and supported tumor formation. Next, the mechanistic study revealed that gp96 upregulated NR5A2 at the protein level, which is a key

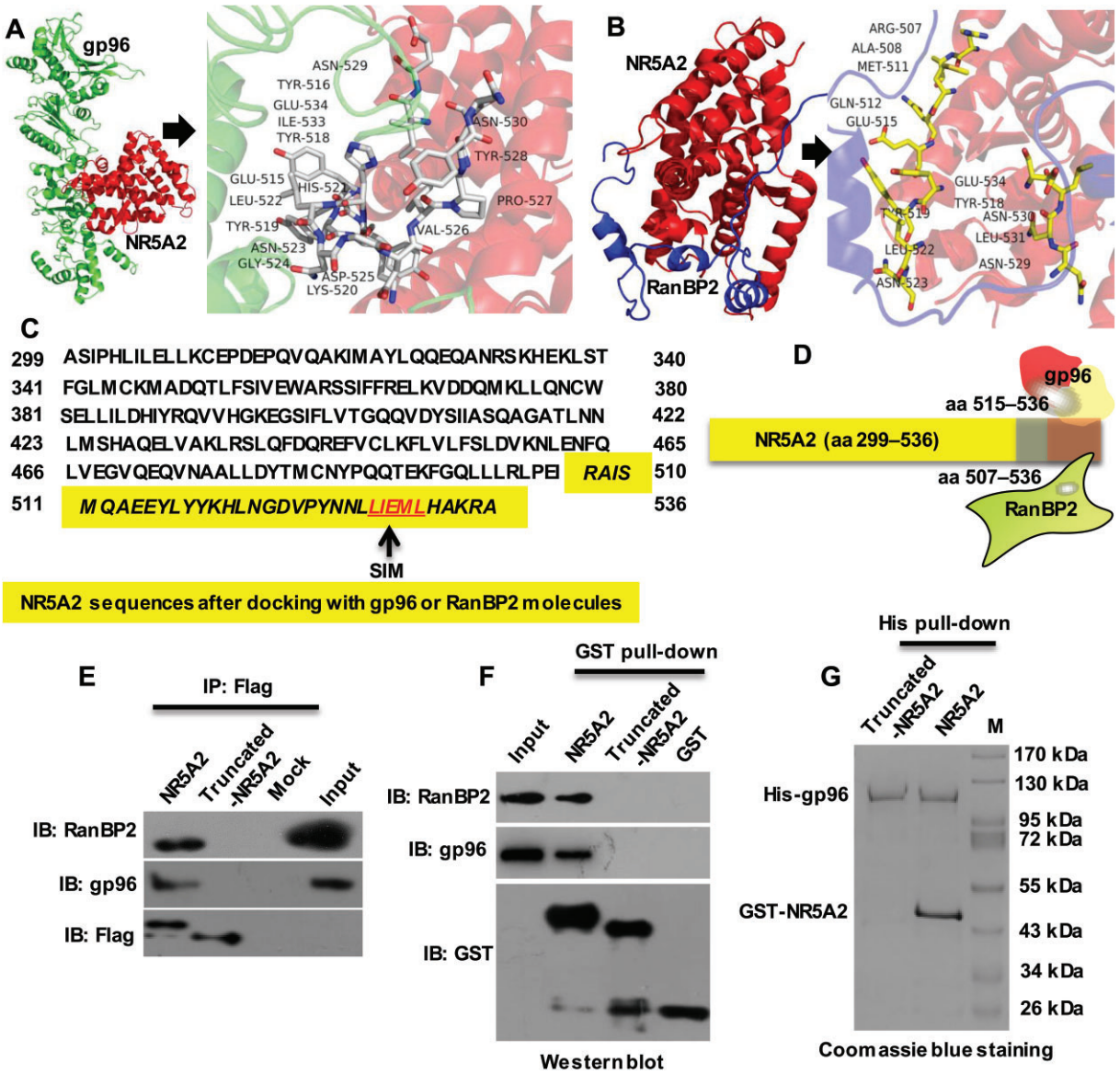

Figure 6 Analysis of the binding sites of gp96 and RanBP2 in NR5A2 protein. (**A** and **B**) Cartoon representation of gp96 (**A**) or RanBP2 (**B**) docking model with NR5A2. Gp96, RanBP2, and NR5A2 residues are in green, blue, and red, respectively. The interaction amino acids are shown as white (between gp96 and NR5A2) or yellow (between RanBP2 and NR5A2) sticks, and non-carbon atoms are colored according to the chemical identity (C, white or yellow; O, red; N, blue; H, wheat). (**C**) The amino acid sequence of NR5A2 (aa 299–536). The putative binding sites in NR5A2 LBD for gp96 and RanBP2 are indicated using italics and bold letters. (**D**) Cartoon figure showing interaction regions in NR5A2 LBD with gp96 and RanBP2. (**E**) Huh7 cells were transfected with pcDNA3.1-Flag-NR5A2 (aa 299–536) (NR5A2), pcDNA3.1-Flag-NR5A2 (aa 299–506) (truncated-NR5A2), or empty vector (mock). After 48 h, cell lysates were immunoprecipitated with Flag antibody followed by immunoblotting for RanBP2, gp96, and Flag. (**F**) Huh7 cell lysates were incubated with GST-NR5A2 (aa 299–536) or GST-NR5A2 (aa 299–506), and the GST pull-down materials were immunoblotted for RanBP2, gp96, and GST. (**G**) Equal amounts of GST-NR5A2 (aa 299–536) and GST-NR5A2 (aa 299–506) were incubated with His-gp96, and the His pull-down materials were subjected to Coomassie blue analysis. All experiments were performed at least three times with similar results.

transcription factor for the AFP gene. Furthermore, RanBP2 was identified as an NR5A2-associated protein with SUMO1 E3 ligase activity, and gp96 could block their interaction by competitively binding to the same sites in NR5A2. Finally, the clinical data from HCC patients showed that gp96 expression in the tumor was positively correlated with AFP levels in serum. Figure 8 illustrates the gp96–NR5A2–RanBP2 regulatory pathway that elevates AFP expression in HCC. According to this model, RanBP2 promotes ubiquitination and proteasomal degradation of NR5A2 by SUMOylation in normal liver tissue and certain HCC with low

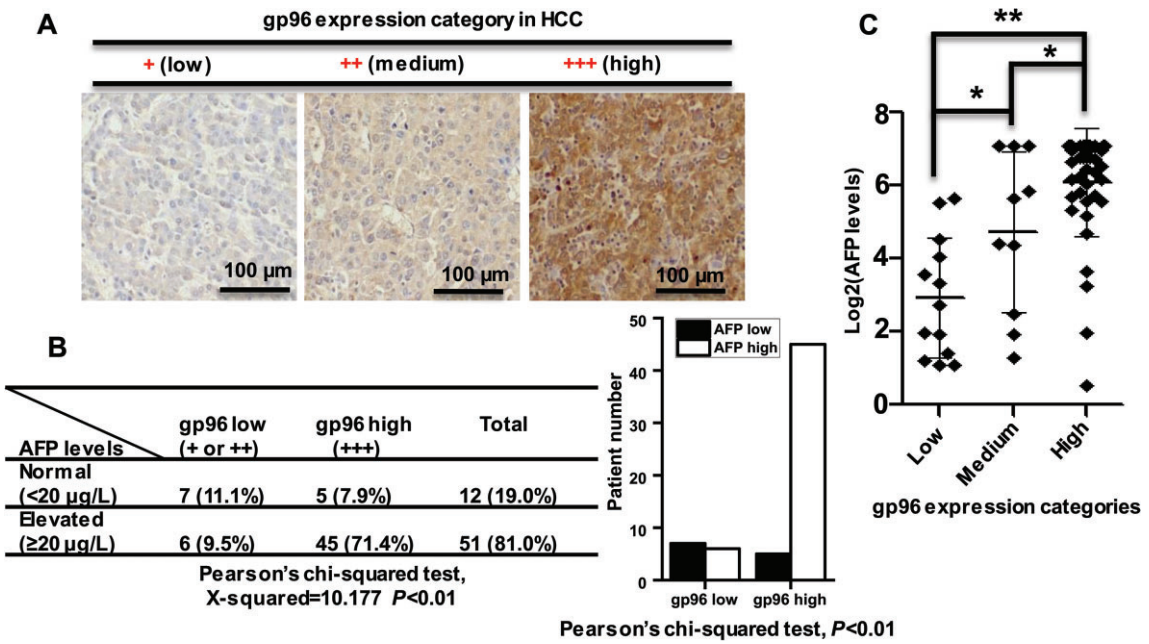

Figure 7 Correlation of gp96 expression in tumors and serum AFP levels in HCC patients. (**A**) IHC analysis of gp96 expression in primary HCC tissues. Representative images indicate immunostaining intensities of 1+, 2+, and 3+. (**B**) The correlation between gp96 expression and serum AFP levels in HCC patients was analysed by Pearson's chi-squared test. Distribution of normal and elevated serum AFP levels in tumors with low and high gp96 expression is shown. (**C**) Higher gp96 expression categories correlate with higher serum AFP levels in HCC patients.

cellular gp96 expression, thereby halting NR5A2-induced AFP expression. On the contrary, in HCC with high gp96 expression, gp96 increases AFP transcription by blocking the interaction between NR5A2 and RanBP2. Our results provide new insight into the distinct status of AFP expression in HCC and might help to design AFP-based HCC diagnosis and disease monitoring approaches with enhanced sensitivity and specificity.

NR5A2 is a member of the nuclear receptor NR5A subfamily (Fayard et al., 2004; Sun et al., 2021). It contains several lysine residues that are modified with SUMOylation by SUMO E3 ligases (Lee et al., 2016; Liu et al., 2021a). SUMOylation regulates the transcriptional activity and subnuclear localization of NR5A2. SUMO modification might also regulate the stability of transcription factors by affecting the subsequent ubiquitination process through cross-talk with ubiquitin (Lee et al., 2016; Rosonina et al., 2017). However, SUMO E3 ligases involved in the SUMOylation of NR5A2 are still unknown. In this study, we demonstrated that RanBP2 acts as a SUMO E3 ligase that binds to and targets NR5A2 for SUMOylation. We further defined its binding sites in NR5A2. RanGAP, HDAC4, and TOP2A have been reported as the SUMOylation targets of RanBP2 (Kirsh et al., 2002; Dawlaty et al., 2008; Werner et al., 2012). Since all the identified RanBP2 target proteins, including RanGAP, HDAC4, TOP2A, and NR5A2, are closely associated with cancer development and progression, the exact role of RanBP2 in HCC deserves further investigation (Liu et al., 2020; Blondel-Tepaz et al., 2021).

gp96 belongs to the HSP90 family and is a major chaperone protein in the ER (Marzec et al., 2012). It acts as a master ER chaperone in response to stress, inflammation, and cancer (Wu et al., 2016; Hoter et al., 2018; Duan et al., 2021). It binds to a variety of client proteins, facilitating their folding and directing their maturation, assembly, and export from the ER to cell surface (Marzec et al., 2012; Kim et al., 2021; Cho et al., 2022). It plays a critical role in maintaining ER homeostasis and protein quality control (Marzec et al., 2012). In addition, ER-resident gp96 can be translocated to cell membrane or cytosol (Marzec et al., 2012; Wu et al., 2015; Kim et al., 2021), which may be due to the decreased expression of KDELR1 that is essential for the retention of gp96 in the ER (Hou et al., 2015b). We and others found that cell membrane or cytosolic gp96 binds to and stabilizes multiple cancer-related proteins, including pro-ADAMTS9, uPAR, HER2, EGFR, ER-α36, and p53, thereby promoting tumor growth, anti-apoptosis, and invasion (Koo and Apte, 2010; Hou et al., 2015a, b; Li et al., 2015; Wu et al., 2015; Duan et al., 2021; Niu et al., 2021). In this study, we uncovered that gp96 interacts and stabilizes NR5A2 by sterically blocking the SUMO E3 ligase RanBP2 binding to NR5A2 and protecting against SUMOylation-induced NR5A2 degradation. We consider that the interaction between gp96 and NR5A2 occurs in the cytoplasm, as NR5A2 exists in both the nucleus and cytoplasm, whereas RanBP2 is localized at the cytoplasmic periphery of the nuclear pore complex (Delphin et al., 1997; Shi et al., 2018). A similar regulatory mechanism involving gp96 was observed for TOP2A, which is a RanBP2 substrate and also a gp96 client protein, but not observed for HDAC4, which is a RanBP2 substrate but does not interact with gp96. Since ubiquitin and SUMO-related modifications determine the fate of the modified proteins, including

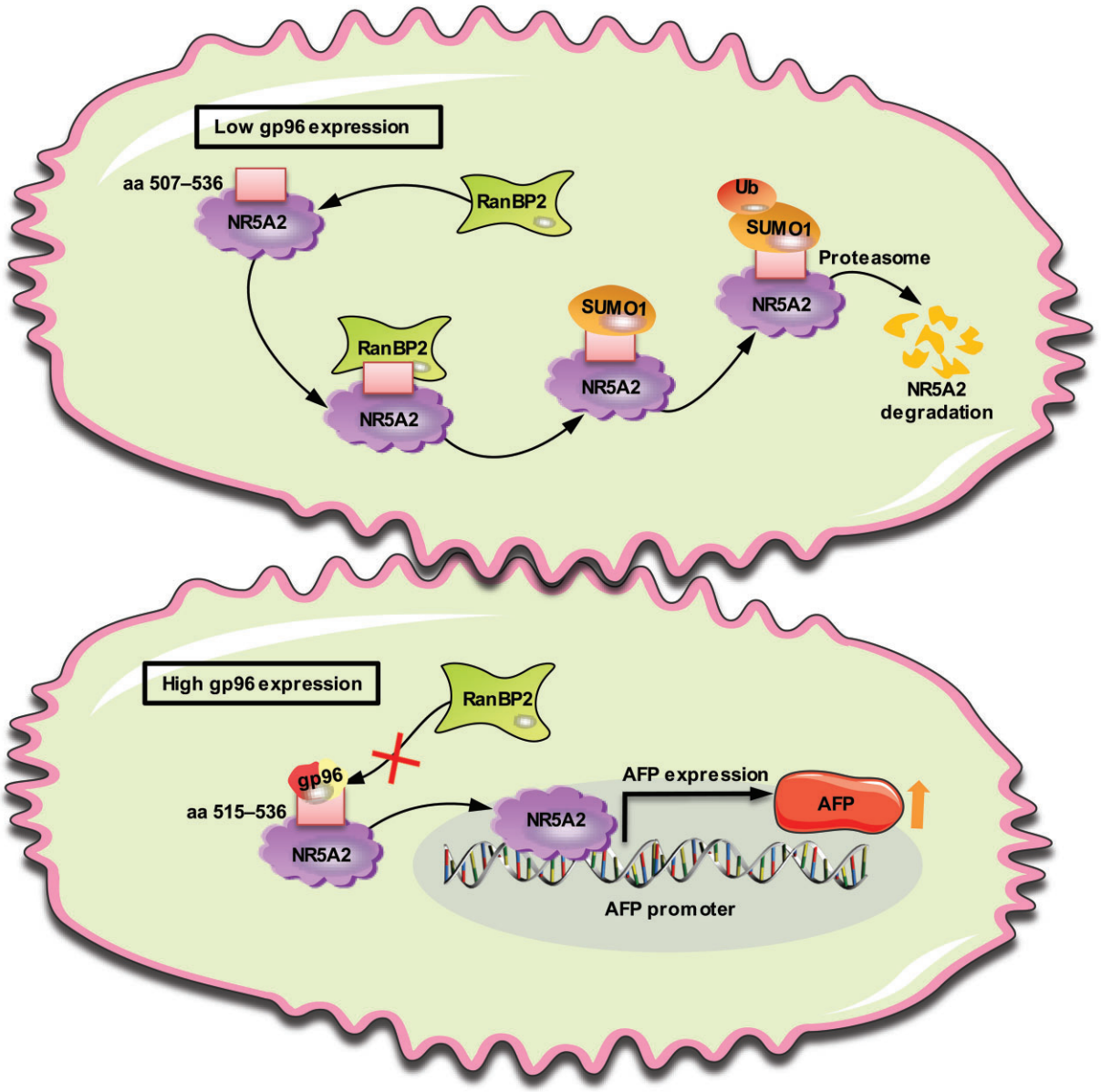

Figure 8 Schematic figure of gp96 promoting AFP expression in HCC. Upper: SUMOylation of NR5A2 by RanBP2 leads to its ubiquitination and subsequent proteasomal degradation. Lower: cellular gp96, with elevated expression in HCC, binds to NR5A2 at the sites spanning from aa 507 to aa 536, which overlap with the RanBP2-binding sites. The binding of gp96 sterically hinders the interaction between RanBP2 and NR5A2, thereby protecting NR5A2 from SUMOylation and degradation. Thus, NR5A2 binds to the AFP promoter and enhances its expression.

their proteasomal degradation, it is worthwhile to explore the effects of gp96 on the stability of its client proteins. We found that gp96 directly controls the interaction between the bound proteins and their E3 ubiquitin/SUMO ligases via the same or overlapping binding sites.

Cellular gp96 expression is controlled mainly by heat shock transcription factors, e.g. ATF4 (Fan et al., 2014). Our previous study showed that hepatitis B virus (HBV) x protein could increase gp96 expression by enhancing the binding of NF-κB to the gp96 promoter (Fan et al., 2013). gp96 expression is elevated in malignant hepatocytes with the progression of HCC (Fan et al., 2013). gp96 levels in tumors are associated with intrahepatic metastasis, degree of tumor differentiation, tumor size, and the predicted outcome of patients (Chen et al., 2014; Ji et al., 2019). High expression of cell membrane gp96 in tumors correlates with the pathogenesis and poor prognosis of HCC in patients (Hou et al., 2015b). These studies indicate the potential of gp96 as a prognostic indicator for HCC. Simultaneously, AFP expression levels also increase with the progression of HCC (Sauzay et al., 2016; Galle et al., 2019). AFP levels in serum have been correlated with HBV infection, tumor size, poor differentiation, and invasion of blood vessels (Sauzay et al., 2016; Galle et al., 2019; Zheng et al., 2020). HCC patients with tumor metastasis have the highest levels of serum AFP

(Trevisani et al., 2001; Piñero et al., 2020). Thus, it can be concluded that AFP is closely associated with the poor prognosis of HCC patients (Berry and Ioannou, 2013; Sauzay et al., 2016; Galle et al., 2019). The identified AFP transcription factors include NR5A2, Nkx2.8, and RAR, while its transcriptional repressors include ZHX2 and ZBTB20 (Kajiyama et al., 2006; Peterson et al., 2011; Sauzay et al., 2016). In the present study, we demonstrated that gp96 upregulates AFP gene expression via NR5A2-induced transcription. Clinical data of HCC patients showed that AFP levels in serum positively correlated with gp96 expression in tumor tissues, and the majority of HCC patients with low gp96 expression exhibited normal AFP levels (Figure 7). Hence, we tentatively defined two distinct HCC subtypes: low gp96 expression with normal AFP, and high gp96 expression with elevated AFP. This finding indicates that low gp96 expression in liver tumors is attributed to normal or minimally increased AFP levels in a substantial proportion of HCC patients.

In conclusion, the current study uncovered a novel mechanism of gp96-mediated upregulation of AFP transcription and expression via NR5A2 in HCC. This mechanism involves the binding of cellular gp96 to NR5A2 and sterically blocking the interaction between NR5A2 and RanBP2, thereby inhibiting NR5A2 SUMOylation, ubiquitination, and subsequent degradation. Furthermore, clinical data of HCC patients revealed two distinct HCC subtypes with high and low gp96 expression, which positively correlate with serum AFP levels. Considering that AFP is the most widely used biomarker in HCC diagnosis and prognosis, our data provide new insights into the regulatory network of AFP expression and might help in designing more precise monitoring approaches for HCC diagnosis and progression.

Materials and methods

Animal studies

Liver-specific gp96KO mice were presented by Prof. Zihai Li and generated by crossing *Albumin-Cre* mice with *Hsp90b1*$^{flox/flox}$ mice to obtain *Albumin-Cre Hsp90b1*$^{flox/flox}$ mice (Rachidi et al., 2015). Genotyping was performed by PCR analysis of genomic DNA obtained from the tail, and the primer sequences used were 5′-TGCCAGAGACTACAATTCCCAGCA-3′, 5′-AAACACGAACTCACCAATCGTGCC-3′ (*Hsp90b1*$^{flox/flox}$ mice), 5′-TGGCAAACATACGCAAGGG-3′, and 5′-CGGCAAACGGACAGA AGCA-3′ (*Albumin-Cre* mice). Fifteen days after birth, gp96KO and heterozygous (Het) mice were intraperitoneally injected with DEN at a dose of 25 mg/kg. Mice were sacrificed after 8 months, and livers were excised. Externally visible tumors ($\geq$1 mm) in the livers were counted, and the liver tissues were stored at −80°C. All animals received human care, and the mouse study was conducted in strict accordance with the protocols approved by the Research Ethics Committee of Institute of Microbiology, Chinese Academy of Sciences (PZIMCAS2011001).

Molecular docking

The crystal structures of NR5A2 LBD from the docking model of NR5A2 DBD–LBD were obtained from PDB-Dev (PDBDEV_00000035) (Seacrist et al., 2020). The crystal structure of full-length gp96 (PDB code 5ULS, residues 48–754) contained three major domains: N-terminal, middle, and C-terminal (Huck et al., 2017). The crystal structure of the SUMO-RanGAP1–Ubc9–Nup358 complex was reported previously (PDB code 1Z5S) containing RanBP2 residues 2631–2711 (Reverter and Lima, 2005; Gareau et al., 2012). The gp96–NR5A2 and NR5A2–RanBP2 protein–protein docking models were created with ZDOCK Server (version 3.0.2) protein–protein docking, each with a centroid phase with rigid-body docking and an all-atom phase (Pierce et al., 2011). PyMoL was used for further visualization and figure preparation.

Patient specimens

Paraffin-embedded hepatic tumor sections of 63 HCC patients were obtained from the Department of Pathology and Hepatology, The Fifth Medical Centre, Chinese PLA General Hospital, between January 2019 and August 2020. The studied clinical characteristics of the subjects are listed in Table 1. The serological AFP level included in this analysis was obtained from the preoperative measurement before and closest to the date of resection. Endogenous gp96 staining was categorized as low (score 1+), medium (score 2+), and high (score 3+) expression based on the staining intensity and immune reactive cell percentage according to a widely used scoring method (slightly modified) (Hicks and Tubbs, 2005): score 1+, slight and incomplete cell staining of hepatoma cells; score 2+, medium cytoplasm staining in at least 50% of hepatocyte cells; score 3+, high cytoplasm staining in at least 85% of hepatocyte cells. The assessments were carried out blindly by two independent observers.

Statistical analysis

All data were analysed using SPSS software (SPSS Science) and R software (version 4.1.2; http://Rproject.org). Results are reported as mean $\pm$ standard deviation (SD). Differences between mean values were analysed using Student's *t*-test. *P*-values <0.05 were considered statistically significant.

Supplementary material

Supplementary material is available at *Journal of Molecular Cell Biology* online. Complete immunoblotting membranes of all IP and pull-down experiments are supplied in Supplementary Additional file 4.

Acknowledgements

The authors thank Donghong Wang, Xiuge Hou, Zihao Wang, Han Zhang, Yang Li, Xiaolan Zhang, Tong Zhao, Fang Cheng, and Shuman Xie from Institute of Microbiology, Chinese Academy of Sciences for technical help and advice.

Funding

This work was supported by the Strategic Priority Research Program of the Chinese Academy of Sciences (XDB29040000), the Industrial Innovation Team grant from Foshan Industrial

Technology Research Institute, Chinese Academy of Sciences, the National Natural Science Foundation of China (32070163, 81871297, and 81903142), China ATOMIC Energy Authority, Foshan High-level Hospital Construction DengFeng Plan, and Guangdong Province Biomedical Innovation Platform Construction Project Tumor Immunobiotherapy.

Conflict of interest: none declared.

Author contributions: S.M., L.Q., and C.L. concepted and designed the study. L.Q. and Z.L. performed the experiments. L.Q. and Z.L. collected data and samples. L.Q., S.M., and C.L. performed the statistical analysis and wrote the manuscript. C.L. and S.M. supervised this work. All the authors read and approved the final manuscript.

References

Ansa-Addo, E.A., Thaxton, J., Hong, F., et al. (2016). Clients and oncogenic roles of molecular chaperone gp96/grp94. Curr. Top. Med. Chem. *16*, 2765–2778.

Bernier, D., Thomassin, H., Allard, D., et al. (1993). Functional analysis of developmentally regulated chromatin-hypersensitive domains carrying the α_1-fetoprotein gene promoter and the albumin/α_1-fetoprotein intergenic enhancer. Mol. Cell. Biol. *13*, 1619–1633.

Berry, K., and Ioannou, G.N. (2013). Serum alpha-fetoprotein level independently predicts posttransplant survival in patients with hepatocellular carcinoma. Liver Transpl. *19*, 634–645.

Blondel-Tepaz, E., Leverve, M., Sokrat, B., et al. (2021). The RanBP2/RanGAP1–SUMO complex gates β-arrestin2 nuclear entry to regulate the Mdm2–p53 signaling axis. Oncogene *40*, 2243–2257.

Chen, W., Peng, J., Ye, J., et al. (2020). Aberrant AFP expression characterizes a subset of hepatocellular carcinoma with distinct gene expression patterns and inferior prognosis. J. Cancer *11*, 403–413.

Chen, W.T., Tseng, C.C., Pfaffenbach, K., et al. (2014). Liver-specific knockout of GRP94 in mice disrupts cell adhesion, activates liver progenitor cells, and accelerates liver tumorigenesis. Hepatology *59*, 947–957.

Cho, Y.B., Kim, J.W., Heo, K., et al. (2022). An internalizing antibody targeting of cell surface GRP94 effectively suppresses tumor angiogenesis of colorectal cancer. Biomed. Pharmacother. *150*, 113051.

Dawlaty, M.M., Malureanu, L., Jeganathan, K.B., et al. (2008). Resolution of sister centromeres requires RanBP2-mediated SUMOylation of topoisomerase IIα. Cell *133*, 103–115.

Delphin, C., Guan, T., Melchior, F., et al. (1997). RanGTP targets p97 to RanBP2, a filamentous protein localized at the cytoplasmic periphery of the nuclear pore complex. Mol. Biol. Cell *8*, 2379–2390.

Deutsch, H.F. (1991). Chemistry and biology of α-fetoprotein. Adv. Cancer Res. *56*, 253–312.

Duan, X., Iwanowycz, S., Ngoi, S., et al. (2021). Molecular chaperone GRP94/GP96 in cancers: oncogenesis and therapeutic target. Front. Oncol. *11*, 629846.

Fan, H., Yan, X., Zhang, Y., et al. (2013). Increased expression of Gp96 by HBx-induced NF-κB activation feedback enhances hepatitis B virus production. PLoS One *8*, e65588.

Fan, Q., Mao, H., Wu, C., et al. (2014). ATF4 (activating transcription factor 4) from grass carp (Ctenopharyngodon idella) modulates the transcription initiation of GRP78 and GRP94 in CIK cells. Fish Shellfish Immunol. *38*, 140–148.

Fayard, E., Auwerx, J., and Schoonjans, K. (2004). LRH-1: an orphan nuclear receptor involved in development, metabolism and steroidogenesis. Trends Cell Biol. *14*, 250–260.

Galle, P.R., Foerster, F., Kudo, M., et al. (2019). Biology and significance of alpha-fetoprotein in hepatocellular carcinoma. Liver Int. *39*, 2214–2229.

Gao, R., Cai, C., Gan, J., et al. (2015). miR-1236 down-regulates alpha-fetoprotein, thus causing PTEN accumulation, which inhibits the PI3K/Akt pathway and malignant phenotype in hepatoma cells. Oncotarget *6*, 6014–6028.

Gareau, J.R., Reverter, D., and Lima, C.D. (2012). Determinants of small ubiquitin-like modifier 1 (SUMO1) protein specificity, E3 ligase, and SUMO-RanGAP1 binding activities of nucleoporin RanBP2. J. Biol. Chem. *287*, 4740–4751.

Gurakar, A., Ma, M., Garonzik-Wang, J., et al. (2018). Clinicopathological distinction of low-AFP-secreting vs. high-AFP-secreting hepatocellular carcinomas. Ann. Hepatol. *17*, 1052–1066.

Hicks, D.G., and Tubbs, R.R. (2005). Assessment of the HER2 status in breast cancer by fluorescence in situ hybridization: a technical review with interpretive guidelines. Hum. Pathol. *36*, 250–261.

Hong, F., Liu, B., Chiosis, G., et al. (2013). α7 helix region of αI domain is crucial for integrin binding to endoplasmic reticulum chaperone gp96: a potential therapeutic target for cancer metastasis. J. Biol. Chem. *288*, 18243–18248.

Hoter, A., El-Sabban, M.E., and Naim, H.Y. (2018). The HSP90 family: structure, regulation, function, and implications in health and disease. Int. J. Mol. Sci. *19*, 2560.

Hou, J., Deng, M., Li, X., et al. (2015a). Chaperone gp96 mediates ER-α36 cell membrane expression. Oncotarget *6*, 31857–31867.

Hou, J., Li, X., Li, C., et al. (2015b). Plasma membrane gp96 enhances invasion and metastatic potential of liver cancer via regulation of uPAR. Mol. Oncol. *9*, 1312–1323.

Huck, J.D., Que, N.L., Hong, F., et al. (2017). Structural and functional analysis of GRP94 in the closed state reveals an essential role for the pre-N domain and a potential client-binding site. Cell Rep. *20*, 2800–2809.

Ji, F., Zhang, Y., Zhu, Z.B., et al. (2019). Low levels of glycoprotein 96 indicate a worse prognosis in early-stage hepatocellular carcinoma patients after hepatectomy. Hum. Pathol. *86*, 193–202.

Kajiyama, Y., Tian, J., and Locker, J. (2006). Characterization of distant enhancers and promoters in the albumin–α-fetoprotein locus during active and silenced expression. J. Biol. Chem. *281*, 30122–30131.

Kim, J.W., Cho, Y.B., and Lee, S. (2021). Cell surface GRP94 as a novel emerging therapeutic target for monoclonal antibody cancer therapy. Cells *10*, 170.

Kirsh, O., Seeler, J.S., Pichler, A., et al. (2002). The SUMO E3 ligase RanBP2 promotes modification of the HDAC4 deacetylase. EMBO J. *21*, 2682–2691.

Kojima, K., Takata, A., Vadnais, C., et al. (2011). MicroRNA122 is a key regulator of α-fetoprotein expression and influences the aggressiveness of hepatocellular carcinoma. Nat. Commun. *2*, 338.

Koo, B.H., and Apte, S.S. (2010). Cell-surface processing of the metalloprotease pro-ADAMTS9 is influenced by the chaperone GRP94/gp96. J. Biol. Chem. *285*, 197–205.

Lee, J., Yang, D.J., Lee, S., et al. (2016). Nutritional conditions regulate transcriptional activity of SF-1 by controlling sumoylation and ubiquitination. Sci. Rep. *6*, 19143.

Li, X., Sun, L., Hou, J., et al. (2015). Cell membrane gp96 facilitates HER2 dimerization and serves as a novel target in breast cancer. Int. J. Cancer *137*, 512–524.

Liu, B., Yang, Y., Qiu, Z., et al. (2010). Folding of Toll-like receptors by the HSP90 paralogue gp96 requires a substrate-specific cochaperone. Nat. Commun. *1*, 79.

Liu, W., Zeng, M., and Fu, N. (2021a). Functions of nuclear receptors SUMOylation. Clin. Chim. Acta *516*, 27–33.

Liu, X., Chen, X., Xiao, M., et al. (2021b). RANBP2 activates O-GlcNAcylation through inducing CEBPα-dependent OGA downregulation to promote hepatocellular carcinoma malignant phenotypes. Cancers *13*, 3475.

Liu, X., Liu, J., Xiao, W., et al. (2020). SIRT1 regulates N^6-methyladenosine RNA modification in hepatocarcinogenesis by inducing RANBP2-dependent FTO SUMOylation. Hepatology *72*, 2029–2050.

Marzec, M., Eletto, D., and Argon, Y. (2012). GRP94: an HSP90-like protein specialized for protein folding and quality control in the endoplasmic reticulum. Biochim. Biophys. Acta *1823*, 774–787.

Marzec, M., Hawkes, C.P., Eletto, D., et al. (2016). A human variant of glucose-regulated protein 94 that inefficiently supports IGF production. Endocrinology *157*, 1914–1928.

Niu, M., Xu, J., Liu, Y., et al. (2021). FBXL2 counteracts Grp94 to destabilize EGFR and inhibit EGFR-driven NSCLC growth. Nat. Commun. *12*, 5919.

Peterson, M.L., Ma, C., and Spear, B.T. (2011). Zhx2 and Zbtb20: novel regulators of postnatal alpha-fetoprotein repression and their potential role in gene reactivation during liver cancer. Semin. Cancer Biol. *21*, 21–27.

Pichler, A., Gast, A., Seeler, J.S., et al. (2002). The nucleoporin RanBP2 has SUMO1 E3 ligase activity. Cell *108*, 109–120.

Pierce, B.G., Hourai, Y., and Weng, Z. (2011). Accelerating protein docking in ZDOCK using an advanced 3D convolution library. PLoS One *6*, e24657.

Piñero, F., Dirchwolf, M., and Pessôa, M.G. (2020). Biomarkers in hepatocellular carcinoma: diagnosis, prognosis and treatment pesponse assessment. Cells *9*, 1370.

Pugh, K.W., Alnaed, M., Brackett, C.M., et al. (2022). The biology and inhibition of glucose-regulated protein 94/gp96. Med. Res. Rev. *42*, 2007–2024.

Rachidi, S., Sun, S., Wu, B.X., et al. (2015). Endoplasmic reticulum heat shock protein gp96 maintains liver homeostasis and promotes hepatocellular carcinogenesis. J. Hepatol. *62*, 879–888.

Reverter, D., and Lima, C.D. (2005). Insights into E3 ligase activity revealed by a SUMO-RanGAP1–Ubc9–Nup358 complex. Nature *435*, 687–692.

Rosonina, E., Akhter, A., Dou, Y., et al. (2017). Regulation of transcription factors by sumoylation. Transcription *8*, 220–231.

Sauzay, C., Petit, A., Bourgeois, A.M., et al. (2016). Alpha-foetoprotein (AFP): a multi-purpose marker in hepatocellular carcinoma. Clin. Chim. Acta *463*, 39–44.

Seacrist, C.D., Kuenze, G., Hoffmann, R.M., et al. (2020). Integrated structural modeling of full-length LRH-1 reveals inter-domain interactions contribute to receptor structure and function. Structure *28*, 830–846.

Shi, B., Lu, H., Zhang, L., et al. (2018). A homologue of Nr5a1 activates cyp19a1a transcription additively with Nr5a2 in ovarian follicular cells of the orange-spotted grouper. Mol. Cell. Endocrinol. *460*, 85–93.

Sun, Y., Demagny, H., and Schoonjans, K. (2021). Emerging functions of the nuclear receptor LRH-1 in liver physiology and pathology. Biochim. Biophys. Acta Mol. Basis Dis. *1867*, 166145.

Trevisani, F., D'Intino, P.E., Morselli-Labate, A.M., et al. (2001). Serum α-fetoprotein for diagnosis of hepatocellular carcinoma in patients with chronic liver disease: influence of HBsAg and anti-HCV status. J. Hepatol. *34*, 570–575.

Werner, A., Flotho, A., and Melchior, F. (2012). The RanBP2/RanGAP1*SUMO1/Ubc9 complex is a multisubunit SUMO E3 ligase. Mol. Cell *46*, 287–298.

Wu, B., Chu, X., Feng, C., et al. (2015). Heat shock protein gp96 decreases p53 stability by regulating Mdm2 E3 ligase activity in liver cancer. Cancer Lett. *359*, 325–334.

Wu, B.X., Hong, F., Zhang, Y., et al. (2016). GRP94/gp96 in cancer: biology, structure, immunology, and drug development. Adv. Cancer Res. *129*, 165–190.

Xie, Z., Zhang, H., Tsai, W., et al. (2008). Zinc finger protein ZBTB20 is a key repressor of alpha-fetoprotein gene transcription in liver. Proc. Natl Acad. Sci. USA *105*, 10859–10864.

Xue, J., Cao, Z., Cheng, Y., et al. (2020). Acetylation of alpha-fetoprotein promotes hepatocellular carcinoma progression. Cancer Lett. *471*, 12–26.

Zheng, Y., Zhu, M., and Li, M. (2020). Effects of alpha-fetoprotein on the occurrence and progression of hepatocellular carcinoma. J. Cancer Res. Clin. Oncol. *146*, 2439–2446.